

Critical current noise investigations in underdamped Josephson devices

C. Granata,^{*} A. Vettoliere,[†] R. Russo, M. Russo, and B. Ruggiero

Istituto di Cibernetica "E. Caianiello" del Consiglio Nazionale delle Ricerche, I-80078 Pozzuoli (Napoli), Italy

(Received 7 July 2010; published 14 March 2011)

An experimental investigation of the critical current noise in underdamped niobium based Josephson devices [junctions and Superconducting Quantum Interference Device (SQUID)] by a technique based on the switching current measurements is reported. By sweeping the junction with a current ramp we measure the critical current switching using the standard time of flight technique and analyze the data to extract the current noise. Measurements on Josephson junctions having an area ranging from (4×4) to (40×40) μm^2 in the temperature range from 4.2 to 1.2 K are reported. The experimental results show a linear behavior of the current white noise from both the junction area and the temperature. These measurements provide very useful information about the intrinsic noise of Josephson devices involving SQUIDs and qubits.

DOI: [10.1103/PhysRevB.83.092504](https://doi.org/10.1103/PhysRevB.83.092504)

PACS number(s): 74.50.+r, 85.25.Cp, 85.25.Dq

One of the most important figures of merit of a Josephson device is the noise, which is typically expressed by the spectral density of the equivalent current, voltage, magnetic flux or field, or charge noise. Due to the extremely intrinsic low noise, the Josephson devices (in particular Superconducting Quantum Interference Devices, SQUIDs) have been employed in many applications like biomagnetism, metrology, magnetic microscopy, astrophysics, nanomagnetism, quantum computing, and particle physics.¹ The importance of the noise in Josephson devices has stimulated many theoretical and experimental investigations leading to an exhaustive comprehension of the main mechanisms responsible for the different noise.² Theories for voltage, current, and magnetic flux noise in resistively shunted junctions, rf SQUID and dc SQUID, have been developed² as well as quantum charge noise in a Cooper pair box.³ In recent years many theoretical⁴⁻⁷ and experimental⁸⁻¹¹ investigations have been devoted to the understanding the low frequency noise in a Josephson device. Such a kind of noise is a very interesting issue since it is related to the decoherence time in Josephson qubits.¹² However, while there are many experimental investigations of critical current noise in overdamped Josephson junctions, it is not the same for the underdamped case,⁸ despite the fact that both phase and flux Josephson qubits employ the underdamped junctions.¹³ Furthermore, recently sensors of magnetic flux based on a flux qubit exhibiting an energy sensitivity close to the standard quantum limit have been developed¹⁴ by using underdamped Josephson devices. Therefore, the knowledge of the noise properties of underdamped Josephson junctions can be also useful for the quantum limited detectors. Up to now, direct measurements of white critical current noise were not available.

In this Brief Report, an experimental investigation of the critical current noise in underdamped niobium based Josephson devices by a technique based on the switching current measurements is presented. A digital sampling of the critical current time oscillation is obtained by sweeping the junction with a current ramp out of the superconducting state and measuring the critical current using the standard time of flight technique. In such a way the time critical current function $[I_c(t)]$ is digitally sampled with a sampling frequency f_s given by the ramp frequency. If Δt is the acquisition time, the total sample number is $N = f_s \cdot \Delta t$. The current

fluctuation is $\delta I_c^k = I_c^k - \langle I_c \rangle$ where k is an index which varies from 0 to $N - 1$ and $\langle I_c \rangle = (I_0 + I_1 + \dots + I_{N-1})/N$ is the mean value of the critical current.

However, to obtain the current noise, it is not possible to simply compute the power spectral density (PSD) of the raw data for the following reasons. If we think, for simplicity to the continuous case, the square intrinsic noise is given by the power of the current fluctuation $(\Delta I_c = I_c(t) - \langle I_c \rangle)$, which is $\langle [\Delta I_c(t)]^2 \rangle = \langle I_c^2(t) \rangle - \langle I_c(t) \rangle^2 = \sigma^2$. It is related to the PSD of the critical current fluctuation $S_{\Delta I_c}(f)$ by

$$\langle (\Delta I_c)^2 \rangle = \frac{1}{2\pi} \int_0^{\omega_f} S_{\Delta I_c}(\omega) d\omega, \quad (1)$$

where $\omega_f/2\pi$ is the physical bandwidth of the system, which is different from the bias sweeping (sampling) frequency (in particular, half of the sampling frequency, Shannon-Nyquist theorem), otherwise the total intrinsic noise should strongly depend on the sampling frequency. It is worth noting that σ^2 is also the square of the width at half maximum of the critical current distribution $P(I)$ and it is well known that the σ of the current distribution changes only slightly with varying the sweeping frequency. Since the PSD cannot depend on the bandwidth and the sigma of the switching distribution has a very small dependence on the sweeping frequency, a physical bandwidth of the system ω_f has to be identified. A reasonable assumption is that the physical bandwidth is equal to the plasma frequency of the junction $\omega_p = 2\pi f_p = (2\pi I_c / C \Phi_0)^{1/2}$, where C is the junction capacitance and Φ_0 is the flux quantum. Note that, if the noise is white, from Eq. (1), the PSD of the critical current noise is given by $2\pi\sigma^2/\omega_p$.

In the discrete case, the PSD of the critical current fluctuation $S_{\Delta I_c}(f)$ is given by the module of the fast Fourier transform X_q divided by the total number of samples:

$$S_{\Delta I}(q) = \frac{X_q \cdot X_q^*}{N} \quad X_q = \sum_{k=0}^{N-1} \left[\Delta I_c^k \left(\frac{f_s}{2f_a} \right)^{1/2} \right] \cdot e^{-j \frac{2\pi}{N} kq} \quad (2)$$

$$q = 0, 1, \dots, N-1.$$

The computation of the PSD is based on the Welch method. The normalization term $(f_s/2f_a)^{1/2}$ takes into account the

above considerations and the bias dependence of the plasma frequency $\omega_a(I) = 2\pi f_a = \omega_p [1 - (I/I_c)^2]^{1/4}$ where I is the bias current. In our case the critical current has been evaluated according to the standard fitting of the experimental data of $P(I)$ and the escape rate $\Gamma(I)$ (Ref. 15), whereas the $\omega_a(I)$, has been computed for $I = I_M$ where I_M is the bias current value corresponding to the maximum of the experimental switching probability curve $P(I)$. This assumption $\omega_a(I) = \omega_a(I_M)$ simplifies the calculations without introducing too large errors (10% in the worst case of large junctions). With respect to the other technique where the underdamped junction (biased above the gap voltage) is placed as one arm of a Wheatstone bridge having a SQUID as a null detector,⁸ this technique allows a direct measure of the critical current oscillations.

The analysis has been performed on high quality underdamped Josephson junctions having an area ranging from (4×4) to $(40 \times 40) \mu\text{m}^2$ in the temperature range from 4.2 to 1.2 K. It is worth noting that these Josephson junctions are in the limit in which the Josephson energy greatly exceeds the thermal energy ($2\pi k_B T / I_c \Phi_0 \ll 1$). The sample fabrication process well described in Ref. 16 is based on Nb/Al-AlOx/Nb trilayer niobium technology. The measurement setup is shown in Fig. 1. The junction was biased with a triangular-shaped waveform at a frequency of 100 Hz. The synchronism of the ramp generator was delayed and sent to start input of a time acquisition board having a time resolution of 12 ns. The junction voltage was amplified and sent to a discriminator that provides the stop signal at the time of the switching out of the zero voltage state. The critical current values were obtained by multiplying the current ramp slope dI/dt (measured after each measurement) with the interval time Δt measured by the time acquisition board. The estimated measurement resolution of the critical current is about 1 part in 10^4 , which is essentially limited by the stability of the synchronism signal and of the delay. The measurements were performed in a pumped liquid ⁴He cryostat with two copper and three μ -metal coaxial shielding cans, using a low-noise, battery powered, four-contact current-voltage technique typically used for the acquisition of the current switching distribution.¹⁷ All the electrical connections to room temperature went through

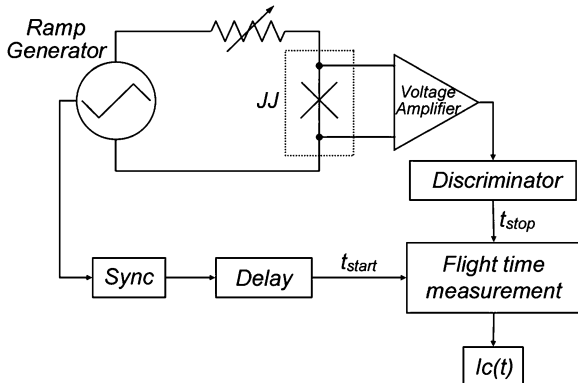


FIG. 1. Experimental setup for the switching current measurements based on a time of flight technique. The resolution of the critical current measurements is about 1 part in 10^4 . The dotted box indicates the cold area.

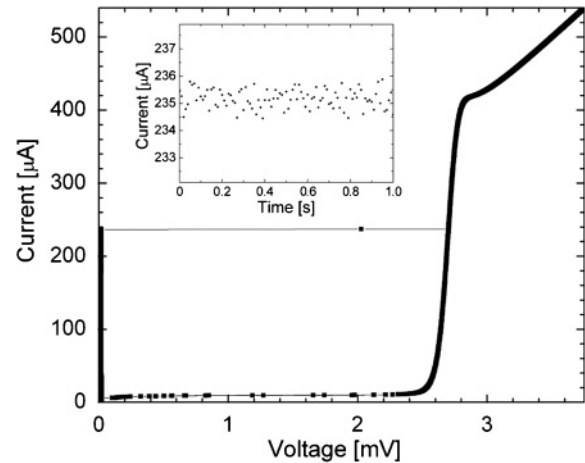


FIG. 2. Current-voltage characteristic of an underdamped Josephson junction having an area of $(20 \times 20) \mu\text{m}^2$ measured at $T = 4.2$ K. The inset shows the values of critical current as a function of the time obtained by biasing the junction with a triangular waveform at 100 Hz.

manganine wires. Between the junction and the manganine wires (in liquid helium), we have employed on each current and voltage leads RC filters (1KOhm and 1nF) calibrated to the bias current of the biggest junction and they were not changed when measuring junctions having a smaller area and lower critical current.

In Fig. 2, a current-voltage characteristic of a $(20 \times 20) \mu\text{m}^2$ Josephson junction measured at $T = 4.2$ K, is reported. The inset shows the critical current oscillation measured with the technique described above by using a biased waveform frequency of 100 Hz. Each measurement includes 100 000 samples corresponding to an acquisition time of 1000 s. For clarity, only a time window of a 1 s is reported in the inset of Fig. 2, so that it is possible to see the single sampling points. In Fig. 3, the current noise spectra of three junctions having an area of (4×4) , (20×20) , and $(40 \times 40) \mu\text{m}^2$ are

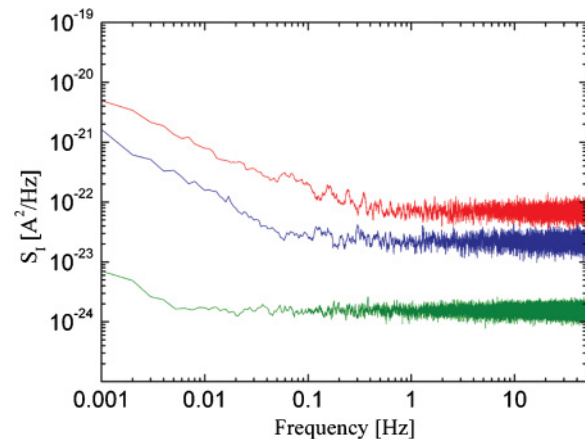


FIG. 3. (Color online) Spectral density of the critical currents relative to three underdamped Josephson junctions measured at $T = 4.2$ K. The junction areas are $16 \mu\text{m}^2$ (green/lower curve), $400 \mu\text{m}^2$ (blue/middle curve), and $1600 \mu\text{m}^2$ (red/higher curve). Each curve has been obtained by averaging the spectral density of 30 different measurements.

reported. They have been obtained by averaging 30 different measurements at $T = 4.2$ K for each junction. An acquisition time of 1000 s has allowed us to reach a frequency as low as a 1 mHz with a resolution of 1 mHz. For each junction, it is possible to observe a white noise and a frequency-dependent noise with a knee depending on the junction size. The white current noise S_{I_c} ranges from 2.0×10^{-24} A²/Hz for the smallest junction to 7.7×10^{-23} A²/Hz for the greatest one. Such values are consistent with the data recently reported in the literature.⁸ As expected, the low frequency noise exhibits a $1/f$ behavior and an inverse proportionality with the junction area. However, the knee position at very low frequency with respect to the data reported in the literature is not clear and it could be due to the employed technique. Note that, as for the recent measurements,⁸ also in our case the current noises $\sqrt{S_{I_c}}$ (1 Hz) of all investigated junctions measured at $T = 4.2$ K are about one order of magnitude less than the value predicted by the empirical formula $[(12 I_c/\mu A)/(A^{1/2}/\mu m)(pA)/Hz^{1/2}]$ obtained by averaging over a wide range of junction areas and critical currents for several different technologies.¹²

We have measured the temperature dependence of the current noise for all the junctions under investigation. In Fig. 4, we report the temperature dependences of the white current noise of a 16 and 100 μm^2 junctions with a linear fit. It is clear from Fig. 4 that the noise linearly scales with both temperatures. It is worth noting that the linear behavior of the current noise as a function of the temperature (Fig. 4) ensures that we are measuring the intrinsic junction noise rather than other noise sources, which could not explain the observed temperature dependence.

Since the noise spectra show essentially a white behavior at a frequency higher than 1 Hz, from Eq. (1), the PSD of the critical current noise is given with a good approximation by $2\pi\sigma^2/\omega_a$. To evaluate σ for all junctions and at all temperatures, the switching current distributions, obtained by making the histograms of the δI_c^k , have been compared with the Buttiker, Harris, and Landauer theory (BHL)¹⁸ in the extremely low damping regime. To compute the BHL curves we have used the experimental parameters and a resistance R

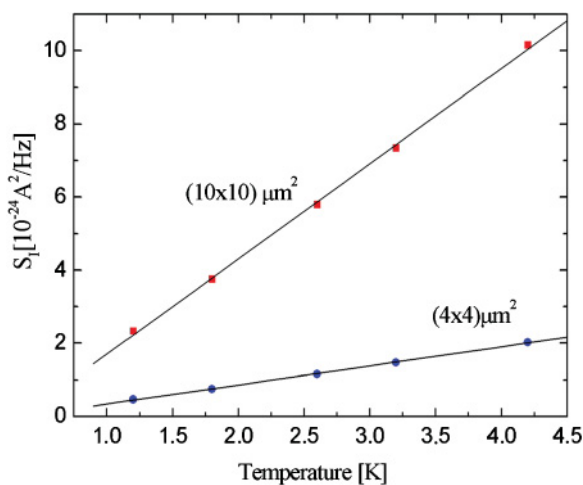


FIG. 4. (Color online) White critical current noise of 16 μm^2 (dots) and a 100 μm^2 (square) underdamped Josephson junctions as a function of the temperature showing a linear behavior.

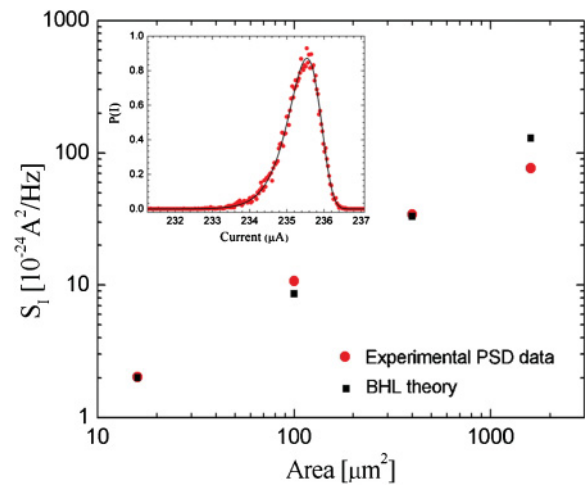


FIG. 5. (Color online) White critical current noise measured at $T = 4.2$ K as a function of the Josephson junction area (red dots) and the values predicted by the BHL theory¹⁸ (black squares). The inset shows a switching current distribution relative to a $(20 \times 20) \mu\text{m}^2$ junction at $T = 4.2$ K (dots), compared to the theory in the extremely low damping regime (black line).

up to a few hundreds ohm, which is the limiting value due to the external circuitry impedance at the plasma frequency. From the BHL curves we can obtain the theoretical standard deviations (σ_{BHL}). In Fig. 5, we report the white current noise as a function of the junction area (red circles) and the predicted values ($2\pi\sigma_{\text{BHL}}^2/\omega_a$) (black squares). The inset shows a switching current distribution relative to a $(20 \times 20) \mu\text{m}^2$ junction at $T = 4.2$ K compared to the BHL theory in the extremely low damping regime (black line).

We have also performed the measurement on an unshunted low critical temperature SQUID. The SQUID loop in a washer configuration includes two junctions having an area of $(4 \times 4) \mu\text{m}^2$. The spectra of the dc SQUID obtained by computing the discrete PSD as a function of the frequency is reported in Fig. 6. It has been obtained by averaging 100 different

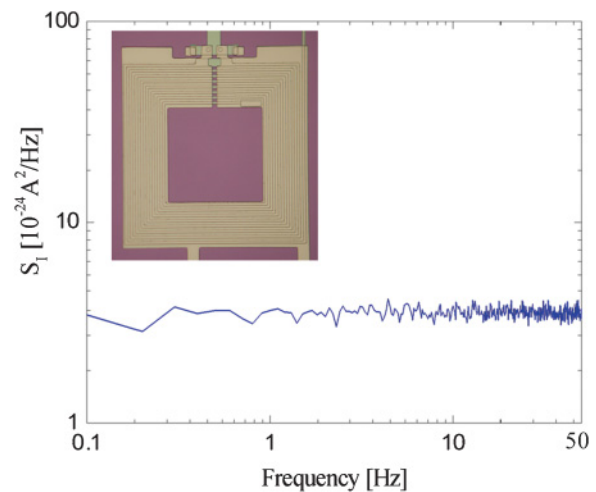


FIG. 6. (Color online) Spectrum of the critical currents relative to an unshunted dc SQUID including two $(4 \times 4) \mu\text{m}^2$ Josephson junctions. The curve has been obtained by averaging the spectral density of 100 different measurements.

TABLE I. Power spectral density of the critical current noise at 4.2 K.

Device	$S_{\Delta I_c}$ (discrete PSD)	$S_{\Delta I_c}(2\pi\sigma_{\text{BHL}}^2/\omega_a)$
JJ 1600 μm^2	$0.8 \cdot 10^{-22} \text{ A}^2/\text{Hz}$	$1.3 \cdot 10^{-22} \text{ A}^2/\text{Hz}$
JJ 400 μm^2	$2.0 \cdot 10^{-23} \text{ A}^2/\text{Hz}$	$3.3 \cdot 10^{-23} \text{ A}^2/\text{Hz}$
JJ 100 μm^2	$1.0 \cdot 10^{-23} \text{ A}^2/\text{Hz}$	$0.9 \cdot 10^{-23} \text{ A}^2/\text{Hz}$
JJ 16 μm^2	$2.0 \cdot 10^{-24} \text{ A}^2/\text{Hz}$	$2.0 \cdot 10^{-24} \text{ A}^2/\text{Hz}$
dc SQUID	$3.5 \cdot 10^{-24} \text{ A}^2/\text{Hz}$	$3.2 \cdot 10^{-24} \text{ A}^2/\text{Hz}$

measurements at $T = 4.2$ K. Each measurement includes 1000 samples corresponding to an acquisition time of 10 s (sweeping frequency of 100 Hz). A picture of the SQUID is shown in the inset of Fig. 6. As expected, the noise of the SQUID is about twice the noise of the single junction having the same area (16 μm^2). It is worth noting that the SQUID was cooling in a double can shield (niobium/cryoperm) guaranteeing a good magnetic shielding and it was not exposed to any external magnetic shield during the measurements. In these circumstances, we do not expect to observe the $1/f$ noise due to the motion of the magnetic flux lines entrapped in the body of the SQUID during the cooldown process, which manifests itself as a flux noise. Furthermore, the SQUID under investigation did not show any junction or inductance asymmetries, so the flux to current transfer factor $\partial I_c/\partial \Phi_e$ was zero for $\Phi_e = 0$. Since, in this case we can assume that the current noise related to the flux noise is $S_{I_c}(f) = S_{\Phi}(f)(\partial I_c/\partial \Phi_e)^2$, if the external magnetic flux is zero it is not

possible to observe the current noise (arising from a flux noise) in any circumstance. We expect a $1/f$ noise arising only from the critical current fluctuations of the two junctions, which, as in the single junction, is not observed in this range of frequency.

In Table I, we report the values of PSD measured at 4.2 K obtained by the discrete PSD (Figs. 4–6), compared with the theoretical predictions ($2p\sigma_{\text{th}}^2/\omega_a$). From the table it is evident that the experimental PSD values are in good agreement with the theoretical predictions indicating the reliability of the measurements.

In conclusion, direct estimation of critical current noise in extremely underdamped niobium based Josephson devices (junctions and SQUID) have been performed. The technique employed is based on the digital sampling of the critical current by switching current measurements and a computation of the PSD, taking properly into account the physical bandwidth ω_a . The experimental data show that the white noise of the critical current scales linearly with the junction area and it has a linear temperature dependence and is in good agreement with the BHL theory. These investigations are very useful for Josephson devices including the underdamped junction like SQUID triggers, phase or flux qubits, and recent interesting applications employing underdamped Josephson junctions as a detector of current noise.¹⁹

This work was partially supported by Italian MiUR under the project “Sviluppo di componentistica superconduttrice avanzata e sua applicazione a strumentazione biomedica” (L 488/92, Cluster 14 – Componentistica Avanzata).

*c.granata@cib.na.cnr.it

†Also with Advanced Technologies Biomagnetics Srl, I-65129 Pescara, Italy.

¹The SQUID handbook: Fundamentals and technology of SQUIDS and SQUID systems, edited by J. Clarke and A. I. Braginski (Wiley, Weinheim, 2006), Vol 2.²The SQUID handbook: Fundamentals and technology of SQUIDS and SQUID systems, edited by J. Clarke and A. I. Braginski (Wiley, Weinheim, 2004), Vol A.³O. Astafiev, Yu. A. Pashkin, Y. Nakamura, T. Yamamoto, and J. S. Tsai, *Phys. Rev. Lett.* **93**, 267007 (2004).⁴R. de Sousa, K. B. Whaley, T. Hecht, J. von Delft, and F. K. Wilhelm, *Phys. Rev. B* **80**, 094515 (2009).⁵L. Faoro and L. B. Ioffe, *Phys. Rev. Lett.* **100**, 227005 (2008).⁶M. Constantin and C. C. Yu, *Phys. Rev. Lett.* **99**, 207001 (2007).⁷R. H. Koch, D. P. Di Vincenzo, and J. Clarke, *Phys. Rev. Lett.* **98**, 267003 (2007).⁸S. Pottorf, V. Patel, and J. E. Lukens, *Appl. Phys. Lett.* **94** 043501 (2009).⁹J. Eroms, L. C. van Schaarenburg, E. F. C. Driessen, J. H. Plantenberg, C. M. Huizinga, R. N. Schouten, A. H. Verbruggen, C. J. P. M. Harmans, and J. E. Mooij, *Appl. Phys. Lett.* **89**, 122516 (2006).¹⁰S. Sendelbach, D. Hover, A. Kittel, M. Muck, J. M. Martinis, and R. McDermott, *Phys. Rev. Lett.* **100**, 227006 (2008).¹¹F. C. Wellstood, C. Urbina, and John Clarke, *Appl. Phys. Lett.* **85**, 5296 (2004).¹²D. J. Van Harlingen, T. L. Robertson, B. L. T. Plourde, P. A. Reichardt, T. A. Crane, and John Clarke, *Phys. Rev. B* **70**, 064517 (2004); see also *Quantum Computing and Quantum Bits in Mesoscopic Systems*, edited by A. J. Leggett, B. Ruggiero, and P. Silvestrini (Plenum, New York, 2004).¹³T. D. Ladd, F. Jelezko, R. Laflamme, Y. Nakamura, C. Monroe, and J. L. O’Brien, *Nature (London)* **464**, 45 (2010); John Clarke and F. K. Wilhelm, *ibid.* **453**, 1031 (2008).¹⁴E. Il’ichev and Ya. S. Greenberg, *Europhys. Lett.* **77**, 58005 (2007).¹⁵J. M. Martinis, M. H. Devoret, and J. Clarke, *Phys. Rev. B* **35**, 4682 (1987).¹⁶C. Granata, C. Di Russo, A. Monaco, and M. Russo, *IEEE Trans. Appl. Supercond.* **11**, 95 (2001).¹⁷B. Ruggiero, C. Granata, V. G. Palmieri, A. Esposito, M. Russo, and P. Silvestrini, *Phys. Rev. B* **57**, 134 (1998), and reference therein; C. Cosmelli, P. Carelli, M. G. Castellano, F. Chiariello, R. Leoni, B. Ruggiero, P. Silvestrini, and G. Torrioli, *J. Supercond.* **12**, 773 (1999).¹⁸M. Buttiker, E. P. Harris, and R. Landauer, *Phys. Rev. B* **28**, 1268 (1983).¹⁹J. T. Peltonen, A. V. Timofeev, M. Meschke, and J. P. Pekola, *J. Low Temp. Phys.* **146**, 135 (2007).